

RESEARCH

Open Access



Towards using fluorescent nanodiamonds for studying cell migration

Claudia Reyes-San-Martin¹, Arturo Elías-Llumbet^{1,2}, Thamir Hamoh¹, Rokshana Sharmin¹, Yue Zhang¹, Angela Hermann¹, Willem Woudstra¹, Aldona Mzyk^{1,3*} and Romana Schirhagl^{1*}

*Correspondence:
aldonamzyk@gmail.com;
romana.schirhagl@gmail.com

¹ Groningen University, University Medical Center Groningen, Antonius Deusinglaan 1, 9713AW Groningen, The Netherlands

² Laboratory of Genomic of Germ Cells, Biomedical Sciences Institute, Faculty of Medicine, University of Chile, Independencia, 1027, Independencia, Santiago, Chile

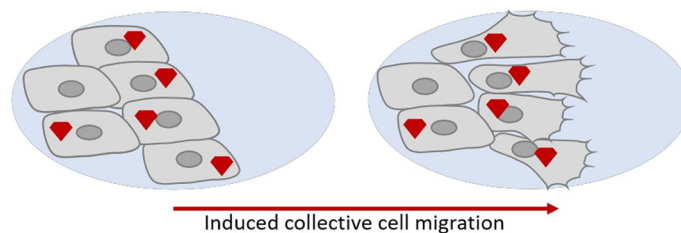
³ Technical University of Denmark, Ørstedes Plads 349, 2800 Kgs., Lyngby, Denmark

Abstract

Since wound healing requires cells to repopulate a damaged area, cell migration is essential. In addition, migration plays a crucial role in cancer metastasis. Whether tumour cells can invade tissue and metastasize is a crucial factor determining their malignancy or in other words a hallmark of cancer (Lazebnik in *Nat Rev Cancer* 10: 232–233, 2010, <https://doi.org/10.1038/nrc2827>). Nanodiamonds potentially offer a powerful tool to investigate these migration processes. Due to their unprecedented photostability, they can function as long-term fluorescent labels. Besides, nanodiamonds are robust quantum sensors that can reveal, for instance, the temperature or the concentration of certain chemicals with nanoscale resolution. However, to utilise nanodiamonds to study cell migration, it is essential to understand if and how the presence of nanodiamonds influences cell migration. Here, we investigate this process for the first time. We found that nanodiamonds do not alter the speed at which HeLa cells populate a scratch at any tested concentrations. Furthermore, we tested cell attachment by quantifying focal adhesion points. Oxygen-terminated fluorescent nanodiamonds influence the cell spreading, the number of focal adhesions and the size of focal adhesion points. Interestingly, this is different for other types of nanodiamonds in the literature. For these particles, it has been described in the literature that they hinder cell migration. Our results support that fluorescent nanodiamonds do not influence cell migration strongly and thus can be used in labelling and sensing migrating cells.

Keywords: Nanodiamonds, Relaxometry, NV centers, Migration, Diamonds

Graphical Abstract



Introduction

Cell migration is crucial for several critical biological processes, including wound healing (Krawczyk 1971) and tissue regeneration (Payne et al. 1996) but also in the formation of cancer metastases and immunity (Seclì et al. 2021; Yamaguchi et al. 2005; Zhu et al. 2015). Cancer invasion and metastasis occurs when cells are spreading from the primary tumour through the circulatory and lymphatic systems, cross the basement membranes and endothelial barriers to colonize distant tissues (Friedl and Wolf 2003; Yang et al. 2010). Cell migration is crucial for this process. Cancer cells possess a broad spectrum of migration and invasion mechanisms, which are similar to migration of other cells and which are crucial for the disease progression (Lazebnik 2010). These include both single and collective cell-migration strategies, which in many tumours can be simultaneously present. Individual cell movement via mesenchymal or amoeboid mode is mediated by cytoskeletal activity without cell–cell interactions with neighbouring cells. Mesenchymal migration involves integrins and matrix-degrading proteases, whereas in amoeboid migration, the interactions with the substrate are weaker. Distinct from single cell motility, collective cell migration occurs as a cell group that retains cell–cell connections and moves co-ordinately. It depends on actin dynamics, integrin based adhesion and proteolytic degradation of extracellular matrix. In collective cell movement mobile cells carry other immobile cell types along (Wu, et al. 2021; Pijuan et al. 2019; Bao et al. 2018; Sheykhzadeh et al. 2020). Depending on the tissue environment, mechanical and biomechanical cues, cancer cells may switch between migration modes. Collective cell migration were studied in-vitro with 2D techniques or 3D techniques with subdivisions for both large categories (Friedl and Wolf 2003; Yang et al. 2010; Bhattacharya et al. 2015). The most commonly known assay is the Boyden chamber. It consists of a transwell chamber in which cells and chemoattractant agents are separated with a porous membrane through which cells can migrate. Although this assay allows to study migratory response of cells to attractants, the method lacks control over geometrical factors and does not allow visual inspection of the migration process. It seems to be better suited for investigation of single cell invasion or migration rather than collective movement (Bouchalova and Bouchal 2022; Yang et al. 2013). To address some of the mentioned limitations, cell exclusion assays were proposed as alternative methods. The wound-healing/scratch assay is a commonly used tool for measuring cell migration rate and polarity (Yang et al. 2010; Bao et al. 2018). The cells are cultured until they form a continuous monolayer. Then part of the cells are scratched from this layer with a pipette tip of a known size. The main disadvantage of wound-healing/scratch assay is that the untouched cells are stressed with cellular components released from scratched cells, including reactive oxygen species (Yang et al. 2010; Bao et al. 2018). In addition, the cells on the border of the scratch may often transiently retract, which affects anoikis, membrane repair and cytokine production. Some disadvantages of the wound healing/scratch assay can be overcome by cell exclusion/barrier assay. In this assay, the cell-free area is made with a removable artificial physical barrier in the cell monolayer. The better defined shape of the barrier, makes this method more reproducible.

Nanoparticles potentially offer a powerful labelling tool to investigate described migration processes. However, many nanoparticles influence cell migration (primarily by slowing it down) (Yang et al. 2010; Bao et al. 2018; Sheykhzadeh et al. 2020; Bhat-tacharya et al. 2015). Gold particles (0.005–0.02 nM), for example, reduced human dermal fibroblast or prostate cancer cell mobility drastically (Yang et al. 2013). Ali et al. have shown that targeting gold nanoparticles (0.1–5 nM) to the nucleus almost entirely inhibits cell migration (Ali et al. 2017). Similarly, zinc sulphate (up to 400 µg/mL) reduced cell migration in breast cancer cells (Tran et al. 2016) or silver nanoparticles (100–500 nM) reduced migration of endothelial cells (Kalishwaralal et al. 2009). Copper nanoparticles (1–10 mM), on the other hand, increased cell migration (Alizadeh et al. 2019), whereas iron oxide nanoparticles have specifically promoted the migration of mesenchymal stem cells (Li et al. 2019). In general, the effect on migration strongly depends on the cell type and the type of nanoparticle. While detonation nanodiamonds (DNDs) and nanodiamonds with a specific surface treatment have been shown to reduce cell migration, the effect of oxygen-terminated fluorescent nanodiamonds produced by high pressure high temperature synthesis has not been studied before (Gao et al. 2020; Yi et al. 2017).

Fluorescent nanodiamonds (FNDs) are potentially useful in studying cell migration. Due to their outstanding photostability, they are powerful optical labels (Vaijyanthimala et al. 2012; Yu et al. 2005; Reineck et al. 2016). They are especially useful if long-term labelling is required (Liu et al. 2009; Haziza et al. 2017). In addition, they are well visible with multiple imaging techniques which are needed in correlative microscopy (Hemelaar et al. 2017a). In addition, diamond defects change their optical properties based on their magnetic surroundings (Schirhagl et al. 2014), which means that they can be used to convert a magnetic resonance signal into an optical signal. As a result, they can be used to sense magnetic resonances (Vaijyanthimala et al. 2012), temperature (Kucsko et al. 2013; Tsai et al. 2015; Sage et al. 2013), strain or electric fields (Dolde et al. 2011). Most impressive is the high sensitivity that can be achieved this way which enables single spin detection (Mamin et al. 1979; Cujia et al. 2019; Staudacher et al. 1979).

Nanodiamonds are taken up by many mammalian cells and have been shown to be non-toxic in many different cell types (in the µg/mL range that is typically used) (Liu et al. 2007; Vaijyanthimala et al. 2009; Paget et al. 2014; Faklaris et al. 2008). However, apart from being non-toxic, it is also crucial that they do not alter the process one needs to study. This has been investigated for the generation of oxidative stress (Hemelaar et al. 2018), cell division (Morita et al. 2020), the cellular ageing process (Laan et al. 2018) or genetic factors which indicate stress (Mytych et al. 2014).

To be useful for cell migration studies, it is essential to determine if and how the presence of nanodiamonds alters the migration behaviour. Here, we evaluate the effect of oxygen-terminated fluorescent nanodiamonds on migration for the first time. Figure 1 summarises the experiments that were conducted in this article.

Materials and methods

Reagents and materials

HeLa cells, high glucose *Dulbecco's Modified Eagle's Medium* (DMEM, Catalog number: 11965092, *Gibco*), Foetal Bovine Serum (FBS, *Sigma Aldrich*), penicillin and streptomycin (*Life Technologies*), phosphate-buffered saline (PBS, *Invitrogen*), trypsin/EDTA

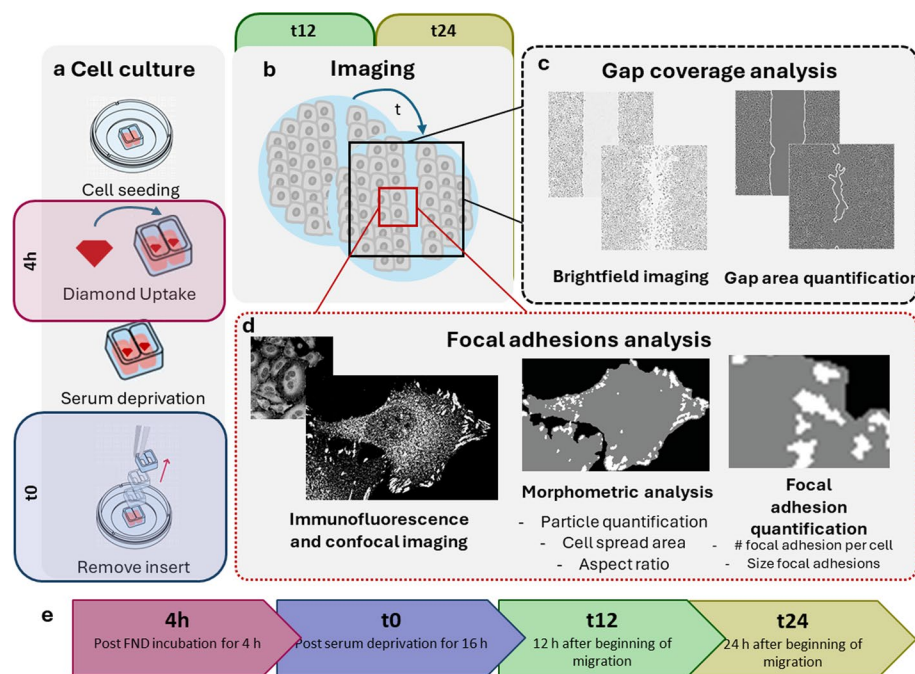


Fig. 1 Schematic representation of methodology applied. **a** HeLa cells are first seeded and cultured in the presence of an insert. Then the insert is removed, leaving behind a gap and cells ability to migrate into this gap was analysed by **b** imaging, **c** gap coverage analysis, **d** focal adhesions quantification and **e** a scheme of the timepoints evaluated during this experiment

(Life Technologies), Fibronectin human plasma (Sigma Aldrich), paraformaldehyde (Merck), triton X-100 (Sigma Aldrich), bovine serum albumin (Sigma Aldrich), mouse-anti-human vinculin monoclonal antibody (clone hVIN-1, Sigma Aldrich), mouse-anti-human talin monoclonal antibody (clone TA205, Invitrogen), goat-anti-mouse IgG/IgM antibody conjugated with fluorescein isothiocyanate (FITC, 115-095-068, Jackson), 4',6-diamidino-2-phenylindole (DAPI, Sigma Aldrich), T75 flask (Greiner), 2-Wells insert (Ibidi), 35 mm glass-bottom dish (Greiner), 12-well plates (Greiner). InviTrap Spin Universal RNA Mini Kit (Strattec molecular, GmbH, Berlin, Germany, <https://www.invitek-molecular.com/>). iScript Advanced cDNA Synthesis Kit (Bio-Rad, Hercules, CA, USA, <https://www.bio-rad.com/>). SsoAdvanced Universal SYBR Green Supermix (Bio-Rad, Hercules, CA, USA). Primers from ThermoFisher: TLN1 (TLN1-S1, GTGCCATTCCAGCCAATGCA; TLN1-A1, CAGAAGGCTTTGGTAGTGGCA), VCL1 (VCL-S, CCAGAACCTCATGCAGTCTGT; VCL-A, GGTATGGTTGGCAGCAACATG), hCypA (hCypA-up, TTGAGCTGTTTGCAGACA; hCypA-down; ACCCGTATGCTTTAGGAT (Brown et al. 2011). 70 nm fluorescent nanodiamonds obtained via high-pressure high-temperature (HPHT) synthesis were purchased from Adamas Nanotechnology, USA. In the last step of their production, the FNDs were cleaned with oxidising acids. This resulted in the formation of oxygen terminal groups on the FND surface. The particles were irradiated by the vendor with an electron beam at 3 MeV to 5×10^{19} e/cm² fluence followed by high-temperature annealing above 600 °C under vacuum for 2 h (Shenderova et al. 2019). As a result, each particle hosted approximately

300 nitrogen-vacancy centres. Their general biocompatibility has been tested, and particles have been extensively characterised in the literature (Faklaris et al. 2008; Ong et al. 2018).

HeLa culture conditions

HeLa cells were used in this study because they are widely available and there is a lot of knowledge about them available from the literature. Furthermore, they are relatively straight forward to culture. Cells were maintained in DMEM complete composed of DMEM supplemented with 4.5 g/L glucose, 10% FBS and 1% penicillin and streptomycin in a T75 flask at 37 °C and 5% CO₂. Cells were sub-cultured twice per week at 90% of confluence. *HeLa* cells were rinsed in PBS and detached from the bottom after 2 min treatment with 2 mL trypsin/EDTA at 37 °C. Cells were resuspended in new T75 flasks containing DMEM complete.

Cell exclusion assay

HeLa cells at 90% of confluence were detached using trypsin/EDTA and resuspended in DMEM complete. Cells were counted using a haemocytometer. Then, 15,000 cells were transferred into each well of the 2-Well insert (*Ibidi*) and placed on a 35 mm glass-bottom dish coated with 10 µg/mL human fibronectin, completing 70 µL per well with DMEM complete (Cappiello et al. 2018; Radstake et al. 2023). Cells were incubated for 24 h in DMEM complete at 37 °C and 5% CO₂ until forming a confluent monolayer (30,000 cells per well). At this point, *HeLa* cells were incubated with 70 nm fluorescent nanodiamonds (FNDs) previously resuspended in FBS (final concentration 10%) and then diluted in DMEM. Five different concentrations of fluorescent nanodiamonds (FNDs), ranging from 1 to 100 µg/mL, were utilized in the study. Consistent with a previous protocol, FND stock solutions were sonicated for 10 min and diluted in pure foetal bovine serum (FBS) to prevent the formation of large FND clusters within the cell culture medium (Hemelaar et al. 2017b). Subsequently, FBS-coated FNDs were combined with serum-free medium to achieve the desired FND concentration along with 10% FBS. Cells were then subjected to a 4-h incubation period at 37 °C with 5% CO₂ (Zhang et al. 2021). Negative control experiments involved culturing cells in complete Dulbecco's Modified Eagle Medium (DMEM). After incubation with nanodiamonds, cells were rinsed twice with PBS and cultured in DMEM serum-free (medium without FBS) for 16 h at 37 °C and 5% CO₂. Then the insert was removed using tweezers, and the medium was replaced by DMEM low serum (medium supplemented with 1% FBS).

Brightfield imaging was performed using an *IncuCyte S3 Live-Cell Analysis System*. Cells were maintained for 24 h at 37 °C and 5% CO₂ while images were acquired each 30 min using 4× objective.

Immunofluorescence

HeLa cells were fixed in 4% paraformaldehyde at timepoints 4 h after FNDs incubation step, and 0 h, 12 h and 24 h after the cell exclusion assay had started (once the insert was removed after 16 h of serum deprivation) and were permeabilised in 0.5% Triton X-100 in PBS. After a 30-min blocking step in 0.5% bovine serum albumin (BSA) in PBS, cells were incubated with a mouse anti-human vinculin primary antibody (1:100

dilution) in PBS containing 1% BSA for 1 h at room temperature, or with a mouse anti-human talin primary antibody (1:100 dilution) in PBS containing 1% BSA overnight at 4 °C. Secondary antibody goat-anti-mouse IgG H&L conjugated with FITC (1:500) and DAPI (2 µg/mL) in PBS containing 1% BSA were incubated for 30 min at room temperature. Confocal z-stacks were acquired in *Zeiss LSM780* using a 63xW objective. Images were acquired using lasers in the Excitation/Emission range of 358/461 nm for DAPI, 488/520 nm for FITC and 532/700 nm for FNDs, and a voxel size of 200 × 190 × 190 nm.

Image processing and statistical analysis

Stacks of brightfield images were processed using a homemade script in *Fiji* (*National Institutes of Health*, Bethesda, MD) to detect and segment gap closure areas (Jonkman et al. 2014). Gap closure percentage was calculated based on the difference between the area free of cells at the initial timepoint compared to 2, 12 and 24 h after removing the insert. The gap closure percentage mean and the standard deviation is plotted for different concentrations of FNDs at due timepoints. Confocal images were analysed to detect cell borders and determine the cell spread area. FNDs particles inside cells were quantified in whole stack images based on the methodology previously described by our group (Hemelaar et al. 2018). In short, we used a three-stage process. First, we selected random cells and defined the area of the cells in 3 dimensions. Second, we moulded the volume to resemble the shape of the cell. The outer part of the volume was then excluded from the analysis to not count particles that adhere to the surface. Finally, we counted particles above a specific threshold in *Fiji* (the threshold was determined beforehand from a slide with evenly spread particles and chosen in a way to get 0 for the control samples). From this we directly obtain the number of objects in the specified region.

Focal adhesions analysis was performed in a single slice of the green channel in which focal adhesion points were visible at the bottom cell. The number of particles per cell, cell spread area, number of focal adhesions per cell and size was plotted for different FNDs concentrations at time 0 and 24 h (Horzum et al. 2014).

Ordinary one-way analysis of variance (ANOVA) was performed using *Graphpad Prism 6* between different FNDs concentrations and the control group and between time 0 and 24 h for each group. Statistical significance was considered for a $p < 0.05$ (n.s. $p > 0.05$, * $p < 0.05$, ** $p < 0.01$, *** $p < 0.001$, **** $p < 0.0001$).

Results and discussion

Collective cell migration is a complex process orchestrated by a sequence of biochemical and biomechanical events that require the coordinated action of the cytoskeletal network and adhesion molecules. Many excellent publications present the molecular and biophysical mechanisms of cultured cancer cells migrating on flat, 2D substrates. However, there is not much information about how cells successfully move in a 3D environment of tissues or how collective cell migration is changed during anticancer therapies. Further explorations require access to stable and inert biolabels. Organic dyes and to some extent also quantum dots suffer from photobleaching (Reineck et al. 2016). In addition, many quantum dots are cytotoxic. Fluorescent nanodiamonds are promising probes to overcome the shortcomings of fluorescent dyes or nanoparticles. FNDs possess exceptional optomagnetic properties and, at the same time, can serve as drug

carriers. So far, only a few studies have investigated the impact of nanodiamonds on cell migration. None of them has evaluated HPHT oxygen-terminated FNDs. The surface chemistry of probes plays a crucial role in the composition of formed protein corona (Hemelaar et al. 2017b; Garcia-Bennett et al. 2019; Francia et al. 2019) and, therefore, endocytic uptake as well as nanoparticle trafficking and final destination. The oxygen-termination of FNDs results from treatment with oxidising acids, usually done at the very end of their fabrication. Moreover, the oxygen groups on the surface help to preserve the functionality of shallow NV-centres that provide FNDs with unique optomagnetic sensing properties. Therefore, this variant of nanodiamonds is a very commonly used material. Our previous studies proved that oxygen-terminated FNDs do not affect the viability and metabolic activity of HeLa cells (Hemelaar et al. 2018). Herein, we have examined their effect on the collective movement of HeLa cells by performing a cell exclusion assay and immunofluorescence analysis of focal adhesion points.

Effect of fluorescent nanodiamonds on HeLa collective migration

The cellular response to different concentrations of 70 nm oxygen-terminated fluorescent nanodiamonds was recorded during 24 h, and the gap closure progression was analysed based on the collected data. Brightfield images before and from 0, 12 and 24 h post-FNDs incubation are shown in Fig. 2a. The percentage of gap coverage with respect to time zero is shown in Fig. 2b for different timepoints and concentrations of FNDs. We observed no statistically significant difference in cell migration within 24 h after removing the insert on HeLa cells containing FNDs compared to the control cultures. Moreover, no statistically significant difference was found in the gap closure rate between different concentrations of FNDs. The observed response of HeLa cells exposed

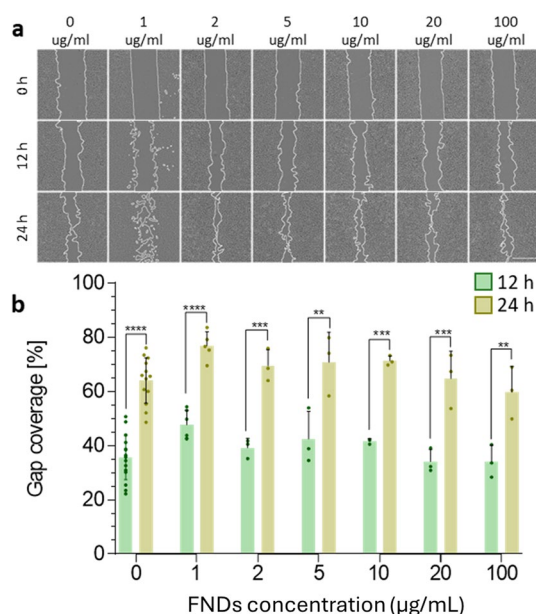


Fig. 2 Effect of fluorescent nanodiamonds on the collective migration HeLa cells. Cell exclusion assay performed in HeLa cells exposed to different concentrations of 70 nm FNDs (0, 1, 2, 5, 10, 20 and 100 µg/mL) shows gap closure rate at 2 time points (12 and 24 h). Error bars shows SD and three experimental replicates are shown. Scale bar 500 µm

to oxygen-terminated FNDs differs from phenomena described for cells treated with detonation (DNDs) or carboxylated HPHT nanodiamonds (cFNDs) from a different source. Gao et al. have shown that 24 h exposure of HeLa to a high concentration of 100 nm cFNDs ($\geq 100 \mu\text{g/mL}$) inhibited their migration (Gao et al. 2020). In parallel, they have evaluated the response of another cancer line, C6 cells, for which cFNDs at a concentration of $25 \mu\text{g/mL}$ have already decreased collective movement. The authors attributed the difference between cell lines to differences in uptake efficiency. The HeLa cells had taken up fewer nanoparticles than C6 cells when they were treated with the same concentration of cFNDs (Gao et al. 2020). The discrepancy between the former results and our paper (both of which use commercially available particles but from different sources) is likely due to differences in exact size distributions, surface chemistry or the presence of different impurities. Such impurities can be for instance different metals that are often found in diamonds from HPHT synthesis. Another impurity that is very common is non-diamond carbon. Wierzbicki et al. have investigated changes in the adhesion, migration, and invasiveness of two glioblastoma cell lines, U87 and U118, in response to DNDs (size of 2–7 nm) (Wierzbicki et al. 2017). Treatment with nanoparticles at a concentration of $50 \mu\text{g/mL}$ caused a twofold reduction in the motility of both cell lines (Wierzbicki et al. 2017).

Similarly, metal nanoparticles can decrease collective migration. Araújo Vieira et al. have reported an inhibitory influence of gold and silver nanoparticles at concentrations below $10 \mu\text{g/mL}$ on the motility of fibroblasts (Vieira, et al. 2017). Tay et al. have shown that after treatment with TiO_2 , SiO_2 , and spherical hydroxyapatite nanoparticles (15–50 nm), TR146 epithelial cells displayed slower migration (Tay et al. 2014). In most of the discussed cases, changes in the migratory behaviour of cells were explained by interactions of nanoparticles with the cytoskeletal network and adhesions proteins. Therefore, in our studies, we have also investigated the latter aspect.

Nanodiamond uptake and distribution in migrating cells

As the endocytosed nanoparticles may interfere with critical components of the cell migration machinery, we have analysed the uptake and distribution of FNDs in HeLa cells (Figs. 3, 4a). We have found that the uptake efficiency of FNDs by HeLa cells increased hundred times after 24 h from the start of the exclusion assay, but only when cells were treated with FNDs at concentration higher than $10 \mu\text{g/mL}$. Moreover, the average number of FNDs per cell has not changed significantly over the 24 h of the migratory experiment. When cells were stimulated to migrate, at times 0 h, 12 h and 24 h post-treatment, FNDs accumulate around the nucleus. For the static HeLa cultures, FNDs could be found not only near the nucleus but also near the membrane. Prabhakar et al. observed that smaller objects were located near the membrane and bigger aggregates (up to $2 \mu\text{m}$) near the nucleus (Prabhakar et al. 2017). Researchers postulated that small FNDs were recycled from the perinuclear area to the membrane to be excreted by cells. The results of our research (Fig. 2) suggest that only a low number of FNDs were possibly recycled to the membrane during the migration process.

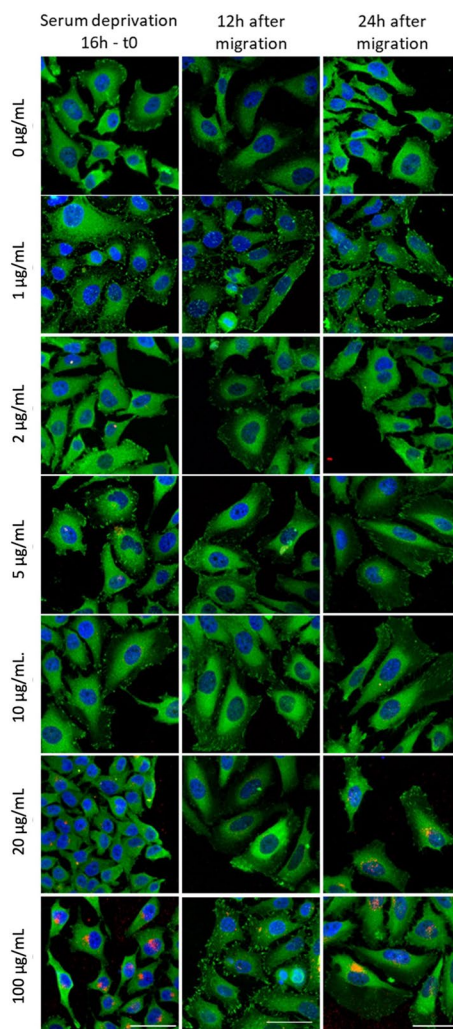


Fig. 3 HeLa cells carry FNDs while they migrate. Migratory HeLa cells exposed to different concentrations of 70 nm FNDs (red dots) over 24 h of cell exclusion assay, were fixed and stained for vinculin (green, focal adhesion protein) and nuclei (blue, DAPI). Scale bar 50 μ m

Effect on cell spreading and focal adhesions

Cells at three timepoints in the experiments before starting the cell exclusion assay (t_0), 12 h after induced migration (t_{12}) and after 24 h after removing the insert (t_{24}), were fixed and immunostained to detect vinculin, a focal adhesion protein involved in migration progression. Confocal images were acquired and analysed to obtain morphometric values such as cell spreading area (Fig. 4b), aspect ratio (Supplementary Fig. 4), and number and size of focal adhesions per cell, as shown in Figs. 3 and 4c, d.

We have found that the shrinking of the cells with time is noticeable for the control condition, while for at least 20 and 100 μ g/mL FND treated cells, the cell spread area increased with time (Fig. 4b; Supplementary Fig. 3b). The number of focal adhesions (Supplementary Fig. 5) shows a similar trend with cell spread area, in which from concentrations higher than 5 μ g/mL of 70 nm FNDs, there are fewer focal adhesion points per cell compared to control at time 0. However, 24 h after starting the

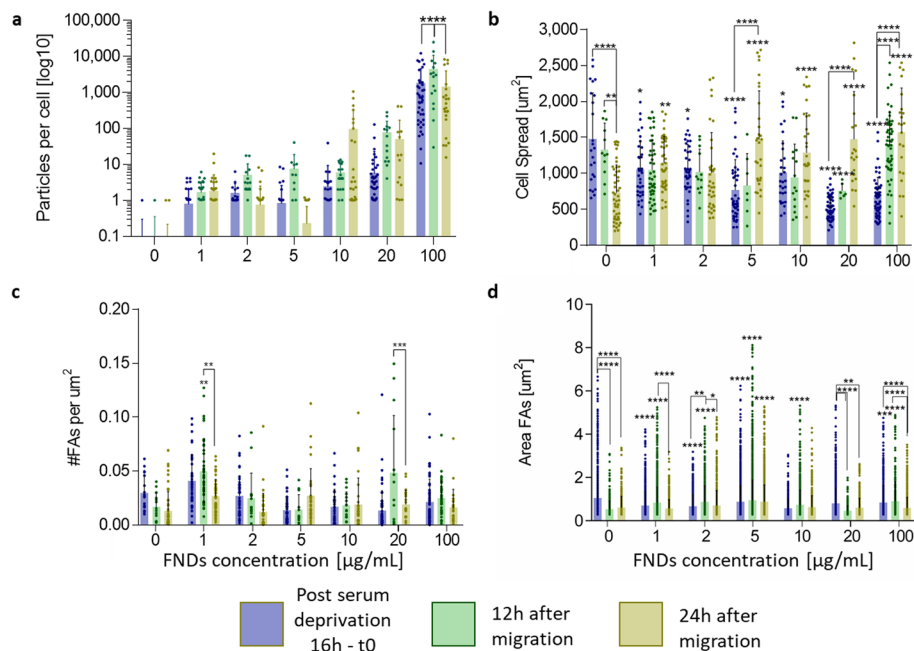


Fig. 4 FND interaction with migratory HeLa cells. **a** uptake efficiency as number of particles per cell and impact on morphometric parameters: **b** cell spreading area, **c** number of focal adhesions per area and **d** size of focal adhesions per condition. Error bars shows SD and three experimental replicates. n.s. $p > 0.05$, * $p < 0.05$, ** $p < 0.01$, *** $p < 0.001$, **** $p < 0.0001$

migration experiment, the number of focal adhesions per cell increased compared to the control without FNDs. This result is influenced by the size of the cells, as no statistically significant difference was found in migratory cells (t0, t12 and t24 h) when the number of focal adhesions is corrected by the area of the cell (Fig. 4c). Except for cells incubated with 1 $\mu\text{g/mL}$ FNDs after 12 h of migration which shows an outstandingly high number of focal adhesions per μm^2 .

On the other hand, we observed statistically significant differences in the size of focal adhesions, showing overall smaller focal adhesions in cells that have taken up particles after 16 h of serum deprivation (t0). 12 h and 24 h after inducing cell migration, the size of vinculin adhesions decreased two times in relation to the initial state. Moreover, cells exposed to FNDs show statistically significantly larger focal adhesion points than cells without FNDs. Similar results were observed for talin expression at 12-h post-migration, indicating changes in talin-mediated focal adhesions. However, at 24-h post-migration, the size of nascent focal adhesions was significantly higher, indicating a complex interplay between talin expression and focal adhesion dynamics over time.

At the transcript level (Supplementary Fig. 7), we observed minimal influence of FND uptake on vinculin or talin expression during cell migration. However, it's noteworthy that at the beginning of the experiment (t0), both vinculin and talin were significantly overexpressed compared to the control across all evaluated concentrations. This overexpression coincides with the 16-h starvation period preceding the experiment, during which cells in the control group also exhibited elevated expression levels.

The observed overexpression of adhesion proteins following starvation suggests a strengthening of adhesion to the surface. Previous studies have shown that starvation

therapy in cancer cells, combined with mesoporous silica shell nanoparticles, upregulates genes related to focal adhesions (Wu et al. 2024).

Overall, these findings underscore the dynamic regulation of focal adhesions in response to various stimuli, highlighting the complexity of cell adhesion and migration processes. In summary, our results have shown that oxygen-terminated FNDs significantly impact the number of vinculin adhesions through higher cell spreading but do not affect the collective migration velocity. The increased mobilisation of the vinculin into focal adhesion complexes and the change in its turnover dynamics requires further investigations. So far, the literature has reported that collective movement was affected by downregulated expression of integrin $\beta 1$, E-cadherin, N-cadherin and vimentin after exposure of the HeLa cells to the cFNDs (Gao et al. 2020). The authors of these studies have concluded that amongst previously listed molecules, vimentin is the most crucial for the cFND-induced attenuation of a cancer cell's ability to migrate. Similarly, Wierzbicki et al. (2017) stated that change in cell migration after treatment with DNDs results from cytoskeleton reorganisation. They have found that nanoparticle uptake resulted in a decreasing amount of stress fibres in the cytoplasm. However, this uptake did not alter adhesion proteins such as vinculin, N-cadherin, and pan-cadherin. In their opinion, endocytosis of nanodiamonds can lead to the internalisation of large areas of the plasma membrane. Therefore, they decrease the availability of receptor tyrosine kinases for binding with their ligands, which normally activates the EGFR/AKT/mTOR signalling pathway. This suggests that FND uptake via endocytosis determines cell migratory behaviour. The process depends on nanoparticle size, shape and surface chemistry and the protein corona composition. Recently this concept became more popular among researchers exploring the effect of the nanoparticle on a collective cell movement.

Sun et al. concluded that the internalisation of PEG-TiO₂ nanoparticles influences cellular motility due to changes in the recycling pattern of integrins, which are the transmembrane receptors responsible for regulating dynamic interactions between the extracellular matrix and the cytoskeleton (Sun et al. 2018). The concept seems to be worthy of further exploration. So far, little is known about how universal the observed phenomena are and what kind of membrane receptors are the key players.

Conclusions

Many other nanoparticles, including carboxylated nanodiamonds used in an earlier study, alter cell migration. However, this is not the case for FNDs. We have demonstrated no significant differences between migrating cells treated with oxygen-terminated FNDs compared to untreated controls regarding collective cell movement. However, we observed that FNDs influence cell spreading, the number of focal adhesions and their size, which is a phenomenon that requires further investigation. While our study was performed on HeLa cells, other types of cells might behave differently. However, the inertness of nanodiamonds has already been shown in many different cell types before. Some applications need to slow down cell migration (for instance, in cancer treatment), while it is crucial for fundamental studies that biolabels or sensing particles do not influence the process that needs to be studied. Thus, our results pave the way for studying migration biology using fluorescent nanodiamonds.

Supplementary Information

The online version contains supplementary material available at <https://doi.org/10.1186/s12645-024-00277-z>.

Supplementary Material 1.

Acknowledgements

RS is thankful to NWO for financial support via a VIDI grant (grant number 016.Vidi.189.002.) and for an ERC starting grant ERC STG-714289.

Author contributions

CRSM performed the experiments in this manuscript with the help of AEL, WW, AH, RSh, TH and YZ. The work was supervised by RSc supported by AM. RS acquired the funding for this project. The manuscript was written by CRSM and edited and approved by all authors.

Funding

RS is thankful to NWO for financial support via a VIDI grant (grant number 016.Vidi.189.002.) and for an ERC starting grant ERC STG-714289.

Availability of data and materials

All data is available in the main manuscript or supplementary material or on request from the authors.

Declarations

Ethics approval and consent to participate

Not applicable.

Consent for publication

All authors have given their consent for publication.

Competing interests

R. Schirhagl is founder of QTsense. The activities of QTsense are not related to the topic of this article. The other authors have no conflicts to declare.

Received: 18 September 2023 Accepted: 18 July 2024

Published online: 10 August 2024

References

- Ali MRK *et al* (2017) Nuclear membrane-targeted gold nanoparticles inhibit cancer cell migration and invasion. *ACS Nano* 11:3716–3726
- Alizadeh S *et al* (2019) Copper nanoparticles promote rapid wound healing in acute full thickness defect via acceleration of skin cell migration, proliferation, and neovascularization. *Biochem Biophys Res Commun* 517:684–690
- Bao YW, Hua XW, Chen X, Wu FG (2018) Platinum-doped carbon nanoparticles inhibit cancer cell migration under mild laser irradiation: multi-organelle-targeted photothermal therapy. *Biomaterials* 183:30–42
- Bhattacharya S *et al* (2015) PEGylated-thymoquinone-nanoparticle mediated retardation of breast cancer cell migration by deregulation of cytoskeletal actin polymerization through miR-34a. *Biomaterials* 51:91–107
- Bouchalova P, Bouchal P (2022) Current methods for studying metastatic potential of tumor cells. *Cancer Cell Int* 22:394. <https://doi.org/10.1186/s12935-022-02801-w>
- Brown C, Morham SG, Walsh D, Naghavi MH (2011) Focal adhesion proteins talin-1 and vinculin negatively affect paxillin phosphorylation and limit retroviral infection. *J Mol Biol* 410:761–777
- Cappiello F, Casciaro B, Mangoni ML (2018) A novel in vitro wound healing assay to evaluate cell migration. *J vis Exp* 2018:e56825
- Cujia KS, Boss JM, Herb K, Zopes J, Degen CL (2019) Tracking the precession of single nuclear spins by weak measurements. *Nature* 571:230–233
- de Vieira LFA *et al* (2017) Metallic nanoparticles reduce the migration of human fibroblasts in vitro. *Nanoscale Res Lett* 12:1–9
- Dolde F *et al* (2011) Electric-field sensing using single diamond spins. *Nat Phys* 7:459–463
- Faklaris O *et al* (2008) Detection of single photoluminescent diamond nanoparticles in cells and study of the internalization pathway. *Small* 4:2236–2239
- Francia V *et al* (2019) Corona composition can affect the mechanisms cells use to internalize nanoparticles. *ACS Nano* 13:11107–11121
- Friedl P, Wolf K (2003) Tumour-cell invasion and migration: diversity and escape mechanisms. *Nat Rev Cancer* 3:362–374. <https://doi.org/10.1038/nrc1075>
- Gao G *et al* (2020) The effect of carboxylated nanodiamonds on tumor cells migration. *Diam Relat Mater* 105:107809
- Garcia-Bennett AE *et al* (2019) Influence of surface chemistry on the formation of a protein corona on nanodiamonds. *J Mater Chem B* 7:3383–3389
- Haziza S *et al* (2017) Fluorescent nanodiamond tracking reveals intraneuronal transport abnormalities induced by brain-disease-related genetic risk factors. *Nat Nanotechnol* 12:322–328

- Hemelaar SR et al (2017a) Nanodiamonds as multi-purpose labels for microscopy. *Sci Rep* 7:720
- Hemelaar SR et al (2017b) The interaction of fluorescent nanodiamond probes with cellular media. *Microchim Acta* 184:1001–1009
- Hemelaar SR et al (2018) The response of HeLa cells to fluorescent nanodiamond uptake. *Sensors (switzerland)* 18:355
- Horzum U, Ozdil B, Pesen-Okvur D (2014) Step-by-step quantitative analysis of focal adhesions. *MethodsX* 1:56–59
- Jonkman JEN et al (2014) An introduction to the wound healing assay using live-cell microscopy. *Cell Adh Migr* 8:440–451. <https://doi.org/10.4161/cam.36224>
- Kalishwaralal K et al (2009) Silver nanoparticles inhibit VEGF induced cell proliferation and migration in bovine retinal endothelial cells. *Colloids Surf B Biointerfaces* 73:51–57
- Krawczyk WS (1971) A pattern of epidermal cell migration during wound healing. *J Cell Biol* 49:247–263
- Kucsko G et al (2013) Nanometre-scale thermometry in a living cell. *Nature* 500:54–58
- Lazebnik Y (2010) What are the hallmarks of cancer? *Nat Rev Cancer* 10:232–233. <https://doi.org/10.1038/nrc2827>
- Le Sage D et al (2013) Optical magnetic imaging of living cells. *Nature* 496:486–489
- Li X et al (2019) Iron oxide nanoparticles promote the migration of mesenchymal stem cells to injury sites. *Int J Nanomed* 14:573–589
- Liu KK, Cheng CL, Chang CC, Chao JI (2007) Biocompatible and detectable carboxylated nanodiamond on human cell. *Nanotechnology* 18:325102
- Liu KK, Wang CC, Cheng CL, Chao JI (2009) Endocytic carboxylated nanodiamond for the labeling and tracking of cell division and differentiation in cancer and stem cells. *Biomaterials* 30:4249–4259
- Mamin HJ et al (1979) Nanoscale nuclear magnetic resonance with a nitrogen-vacancy spin sensor. *Science* 339(2013):557–560
- Morita A et al (2020) The fate of lipid-coated and uncoated fluorescent nanodiamonds during cell division in yeast. *Nanomaterials* 10:516
- Mytych J et al (2014) Nanodiamond-mediated impairment of nucleolar activity is accompanied by oxidative stress and DNMT2 upregulation in human cervical carcinoma cells. *Chem Biol Interact* 220:51–63
- Ong SY et al (2018) Interaction of nanodiamonds with bacteria. *Nanoscale* 10:17117–17124
- Paget V et al (2014) Carboxylated nanodiamonds are neither cytotoxic nor genotoxic on liver, kidney, intestine and lung human cell lines. *Nanotoxicology* 8:46–56
- Payne JM, Cobb CM, Rapley JW, Killoy WJ, Spencer P (1996) Migration of human gingival fibroblasts over guided tissue regeneration barrier materials. *J Periodontol* 67:236–244
- Pijuan J et al (2019) In vitro cell migration, invasion, and adhesion assays: from cell imaging to data analysis. *Front Cell Dev Biol* 7:107
- Prabhakar N et al (2017) Intracellular trafficking of fluorescent nanodiamonds and regulation of their cellular toxicity. *ACS Omega* 2:2689–2693
- Radstake WE et al (2023) Comparison of in vitro scratch wound assay experimental procedures. *Biochem Biophys Rep* 33:101423
- Reineck P et al (2016) Brightness and photostability of emerging red and near-IR fluorescent nanomaterials for bioimaging. *Adv Opt Mater* 4:17604–17605
- Schirhagl R, Chang K, Loretz M, Degen CL (2014) Nitrogen-vacancy centers in diamond: Nanoscale sensors for physics and biology. *Annu Rev Phys Chem* 65:83–105
- Secli L et al (2021) Targeting the extracellular hsp90 co-chaperone morgana inhibits cancer cell migration and promotes anticancer immunity. *Cancer Res* 81:4794–4807
- Shenderova OA et al (2019) Review article: synthesis, properties, and applications of fluorescent diamond particles. *J Vac Sci Technol, b: Nanotechnol Microelectron: Mater, Process, Meas, Phenom* 37:030802
- Sheykhzadeh S et al (2020) Transferrin-targeted porous silicon nanoparticles reduce glioblastoma cell migration across tight extracellular space. *Sci Rep* 10:2320
- Staudacher T et al (1979) Nuclear magnetic resonance spectroscopy on a (5-nanometer)³ sample volume. *Science* 339(2013):561–563
- Sun Q, Kanehira K, Taniguchi A (2018) PEGylated TiO₂ nanoparticles mediated inhibition of cell migration via integrin beta 1. *Sci Technol Adv Mater* 19:271–281
- Tay CY et al (2014) Nanoparticles strengthen intracellular tension and retard cellular migration. *Nano Lett* 14:83–88
- Tran TA, Krishnamoorthy K, Cho SK, Kim SJ (2016) Inhibitory effect of zinc sulfide nanoparticles towards breast cancer stem cell migration and invasion. *J Biomed Nanotechnol* 12:329–336
- Tsai PC et al (2015) Gold/diamond nanohybrids for quantum sensing applications. *EPJ Quantum Technol* 2:1–12
- Vaijayanthimala V, Tzeng YK, Chang HC, Li CL (2009) The biocompatibility of fluorescent nanodiamonds and their mechanism of cellular uptake. *Nanotechnology* 20:425103
- Vaijayanthimala V et al (2012) The long-term stability and biocompatibility of fluorescent nanodiamond as an in vivo contrast agent. *Biomaterials* 33:7794–7802
- Van Der Laan KJ et al (2018) Toward using fluorescent nanodiamonds to study chronological aging in *Saccharomyces cerevisiae*. *Anal Chem* 90:13506–13513
- Wierzbicki M et al (2017) Diamond, graphite, and graphene oxide nanoparticles decrease migration and invasiveness in glioblastoma cell lines by impairing extracellular adhesion. *Int J Nanomedicine* 12:7241–7254
- Wu JS et al (2021) Plasticity of cancer cell invasion: patterns and mechanisms. *Transl Oncol* 14:100899. <https://doi.org/10.1016/j.tranon.2020.100899>
- Wu X et al (2024) NIR-II imaging-guided precise photodynamic therapy for augmenting tumor-starvation therapy by glucose metabolism reprogramming interference. *Sci Bull (beijing)* 69:1263–1274
- Yamaguchi H, Wyckoff J, Condeelis J (2005) Cell migration in tumors. *Curr Opin Cell Biol* 17:559–564. <https://doi.org/10.1016/j.ceb.2005.08.002>

- Yang JX, Tang WL, Wang XX (2010) Superparamagnetic iron oxide nanoparticles may affect endothelial progenitor cell migration ability and adhesion capacity. *Cytotherapy* 12:251–259
- Yang JA, Phan HT, Vaidya S, Murphy CJ (2013) Nanovacuum: Nanoparticle uptake and differential cellular migration on a carpet of nanoparticles. *Nano Lett* 13:2295–2302
- Yi H et al (2017) Nanodiamonds interfere with Wnt-regulated cell migration and adipocyte differentiation in cells and embryonic development in vivo. *Part Part Syst Charact* 34:1600208
- Yu SJ, Kang MW, Chang HC, Chen KM, Yu YC (2005) Bright fluorescent nanodiamonds: no photobleaching and low cytotoxicity. *J Am Chem Soc* 127:17604–17605
- Zhang Y et al (2021) Not all cells are created equal—endosomal escape in fluorescent nanodiamonds in different cells. *Nanoscale* 13:13294–13300
- Zhu G et al (2015) CXCR3 as a molecular target in breast cancer metastasis: Inhibition of tumor cell migration and promotion of host anti-tumor immunity. *Oncotarget* 6:43408

Publisher's Note

Springer Nature remains neutral with regard to jurisdictional claims in published maps and institutional affiliations.